

Boron-Doped Graphene: Scalable and Tunable p-Type Carrier Concentration Doping

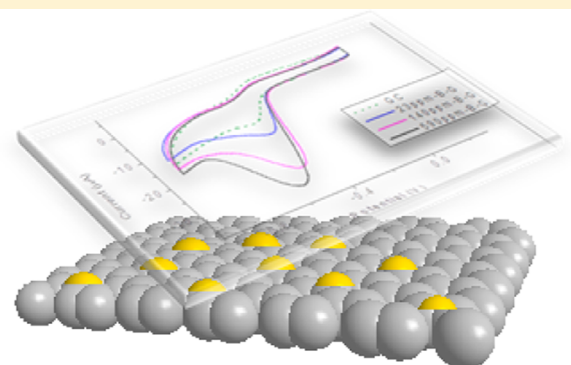
Lu Wang,[†] Zdeněk Sofer,[‡] Petr Šimek,[‡] Ivo Tomandl,[§] and Martin Pumera*,[†]

[†]Division of Chemistry and Biological Chemistry, School of Physical and Mathematical Sciences, Nanyang Technological University, Singapore 637371, Singapore

[‡]Department of Inorganic Chemistry, Institute of Chemical Technology, Technická 5, 166 28 Prague 6, Czech Republic

[§]Nuclear Physics Institute of the ASCR, v.v.i., Řež 130, 250 68 Rež, Czech Republic

ABSTRACT: Precisely engineered changes in Fermi levels of graphene-based materials are of high importance for their applications in electronic and electrochemical devices. Such applications include photoelectrochemical reactions or enhanced electrochemical performance toward reduction of oxygen. Here we describe a method for scalable and tunable boron doping of graphene via thermal exfoliation of graphite oxide in BF_3 atmosphere at different temperatures. The temperature and atmospheric composition during exfoliation influences the kinetics of decomposition of the reactants and levels of doping, which range from 23 to 590 ppm. The resulting materials were characterized by prompt γ -ray analysis, X-ray photoelectron spectroscopy, Raman spectroscopy, and scanning electron microscopy. Recent claims on enhanced catalytic properties of boron-doped graphenes toward the reduction of oxygen were addressed, as well as similar claims on enhanced capacitance.



INTRODUCTION

Doping of graphene with electron-donating or electron-withdrawing groups is important for changing the electronic properties of graphene.¹ Such electron-donating groups include nitrogen^{2–6} or phosphorus,⁷ while electron-withdrawing group include boron.⁸ Doping by electron-donating (n-type, electron donors) or -withdrawing groups (p-type, electron acceptors) changes the electron density of the graphene sheets and as such influences its electrochemical property.⁹ The level of doping is of high importance as carrier density is crucial for tuning the performance of the material. Another important issue with production of doped materials is to produce scalable methods for potentially large quantities of doped materials manufactured. Here we present a technique for scalable production and tunable doping levels by exfoliation of graphite oxide in BF_3 atmosphere at different temperatures. As secondary objective, we investigate the electrochemical properties of such p-doped materials and compare them to the ones found in literature.

It has been claimed that nitrogen-doped graphenes exhibit unusual (as compared to pure graphene) electrocatalytic effects toward reduction of H_2O_2 and oxygen,^{2,6,9} which have very important implications for biosensing and fuel cells applications, respectively. Nitrogen-doped graphenes were also claimed to have large capacitance when compared to graphene. Interestingly, boron-doped graphene was claimed to exhibit similar effects, being electrocatalytic toward oxygen reduction¹⁰ and having increased capacitance in comparison to pure graphene.¹¹ It seems that regardless of the atoms doped in graphene the very

same properties are enhanced.^{2,6,10–12} As such, we wish to further address this issue. In theory, with increased doping of materials with electron-deficient components, the easier would be the oxidation of the compound, while the reduction becomes more difficult.^{13–15} This is contrary to some previous reports on boron-doped graphene catalyzing the electrochemical reduction of oxygen.^{10–12} Here we prepared boron-doped graphene with different concentrations of boron as mentioned above. With detailed characterization using scanning electron microscope, Raman spectroscopy, X-ray photoelectron spectroscopy, and prompt γ -ray analysis, and cyclic voltammetry, we studied how increasing the concentration of boron in graphene influences its electrochemical properties, such as its electrocatalysis toward reduction of oxygen and its capacitance.

RESULTS AND DISCUSSION

Boron-doped graphenes were prepared by thermal exfoliation of graphite oxide in an atmosphere with boron trifluoride diethyl etherate at 1000 °C in N_2/H_2 , 800 °C in N_2 and 1000 °C in N_2 . The graphite oxide underwent exfoliation, deoxygenation (producing H_2O , CO , CO_2 , and more complex organic molecules^{16–19}) and simultaneous doping with boron. The resulting boron-doped graphenes were characterized by prompt γ -ray analysis (PGAA), scanning electron microscopy (SEM), X-

Received: May 25, 2013

Revised: August 29, 2013

Published: October 18, 2013

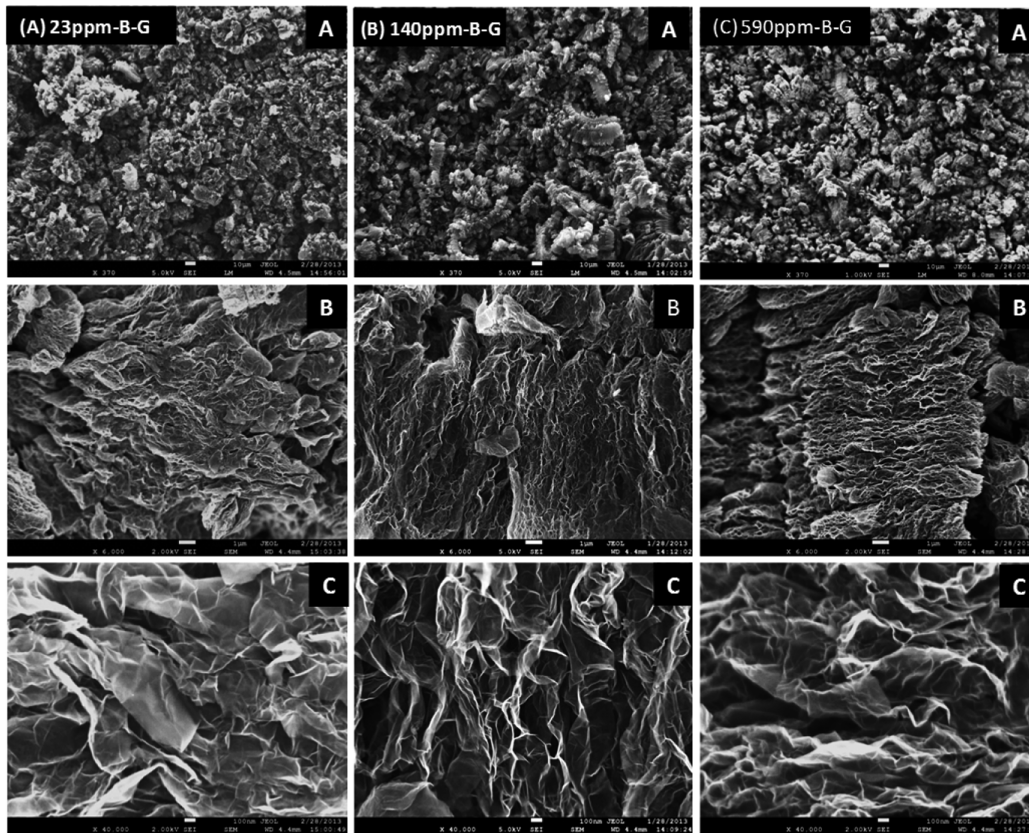


Figure 1. Scanning electron micrographs of boron-doped graphenes containing 23 ppm of B, 140 ppm of B, and 590 ppm of B. Images were obtained at (A) 370 \times , (B) 6000 \times , and (C) 40 000 \times magnifications and scale bars are 10 μ m, 1 μ m, and 100 nm, respectively.

ray photoelectron spectroscopy (XPS), Raman spectroscopy, and cyclic voltammetry (CV) to study their electrocatalytic properties toward oxygen reduction as well as its capacitance. We abbreviate all boron-doped graphenes as B-G in this paper.

First, we investigated whether the thermal shock treatment of graphite oxide in BF_3 atmosphere led into exfoliation of graphite oxide (GO). The morphology of the product, boron-doped graphene (B-G), was studied by SEM. Figure 1 shows the SEM images of boron-doped graphenes that were prepared by exfoliation at 1000 °C in N_2/H_2 atmosphere (containing 23 ppm of B), 800 °C in N_2 atmosphere (containing 140 ppm of B), and 1000 °C in N_2 atmosphere (containing 590 ppm of B). All materials showed a typical exfoliated structure in agreement with previous studies and confirmed successful thermal exfoliation of graphite oxide in BF_3 atmosphere.

Consequently, we study the effect of exfoliation temperature upon level of graphene doping with boron by prompt γ -ray analysis (PGAA). PGAA is an absolute method of determination of trace levels of an element. The absolute content of boron in samples was determined relatively to H_3BO_3 liquid standard with known boron concentration. As shown in Figure 2, it was found that exfoliation of graphite oxide at 1000 °C in N_2/H_2 atmosphere led to doping of graphene at levels of 23 ppm boron, while with exfoliation in nitrogen atmosphere a larger amount of boron was introduced, 140 ppm boron at 800 °C and 590 ppm at 1000 °C. This result clearly shows that, with higher exfoliation temperature, higher amount of boron atoms can be doped into the graphene. Also, we observed the significant decrease of boron concentration for GO exfoliated in atmosphere with hydrogen. Therefore, this result has confirmed successful doping of boron into the graphene sheets.

Having determined the level of doping of graphene with boron, we consequently characterize the defect density in boron-doped graphene using Raman spectroscopy. Figure 3 shows the Raman spectra of three boron-doped graphenes. The D band at approximately 1350 cm^{-1} indicates the presence of defects caused by the sp^3 -hybridized carbon atoms, while the pristine sp^2 lattice carbon atoms in the graphene sheet shows a G band at approximately 1560 cm^{-1} . The ratio between D and G band intensities ($I_{\text{D}}/I_{\text{G}}$) can be used as an indication of the degree of disorder in a carbon structure and the $I_{\text{D}}/I_{\text{G}}$ ratio for 23 ppm B-G, 140 ppm B-G, and 590 ppm B-G are 0.903, 0.632, and 0.732, respectively. The average crystallite sizes (L_a) of the various materials can be estimated based on the D- and G-band intensities by application of the eq 1.²⁰

$$L_a = 2.4 \times 10^{-10} \times \lambda_{\text{laser}}^4 \times I_{\text{G}}/I_{\text{D}} \quad (1)$$

where λ_{laser} is the wavelength of the excitation laser in nanometers and I_{G} and I_{D} are the intensities of the Raman G and D bands, respectively.

We calculated the crystallite sizes in boron-doped graphenes. We found that the L_a of 23 ppm B-G is 18.6 nm, 140 ppm B-G is 26.6 nm, and 590 ppm B-G of is 23.0 nm. All three boron-doped graphenes exhibit both D' band and 2D band at approximately 1620 and 2700 cm^{-1} , respectively, which indicate a low degree of disorder in their carbon structure.

Consequently, we determined the elemental compositions of boron-doped graphenes using XPS. XPS is a chemical analysis method and it is useful to determine not only the elemental composition but also bonding arrangement. The wide scan and C 1s high-resolution XPS of boron-doped graphenes were obtained. The wide scan and high-resolution XPS of C 1s

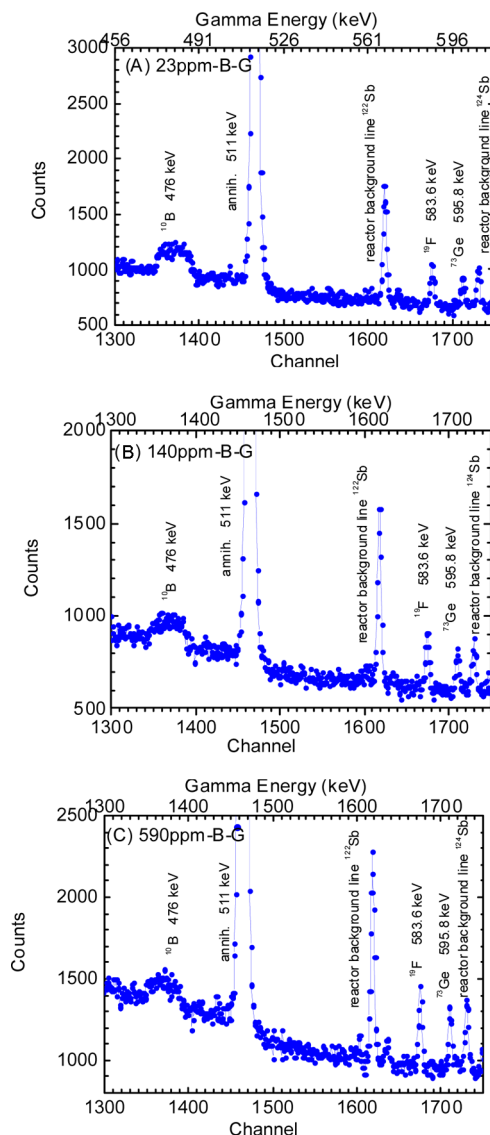


Figure 2. PGAA spectra of boron-doped graphenes containing (A) 23 ppm of B, (B) 140 ppm of B, and (C) 590 ppm of B.

shown in Figure 4 for three graphenes indicate that the oxygen-containing groups were mostly removed and the thermally reduced graphenes were prepared successfully. The C/O ratios obtained from wide scan XPS are 14.2 for 23 ppm B-G, 8.9 for 140 ppm B-G, and 16.1 for 590 ppm B-G. The high-resolution XPS of C 1s signal give insight into the chemical composition of residual oxygen-containing groups, as they show different energy levels, C=C bond of 284.5 eV, C-C bond of 285.6 eV, C-O bond of 286.6 eV, C=O bond of 287.6 eV and O-C=O bond of 289.6 eV. The boron-doped graphenes prepared at 1000 °C in N₂/H₂, 800 °C in N₂, and 1000 °C in N₂ contain 67.0%, 60.8%, and 68.5% of C=C bonds, 14.8%, 18.2%, and 13.9% of C-C bonds, 7.0%, 8.4%, and 6.9% of C-O bonds, 2.4%, 3.0%, and 2.8% C=O bonds, and 8.8%, 9.5%, and 7.9% O-C=O bonds, respectively. Although XPS is not sensitive enough to measure trace amounts of boron, it is highly useful for determination of residual oxygen-containing groups in reduced graphene.

Combustible elemental analysis was also used to determine the elemental composition of the boron-doped graphenes. This method is useful to measure the absolute content of the combustible elements in the bulk material. In combination with

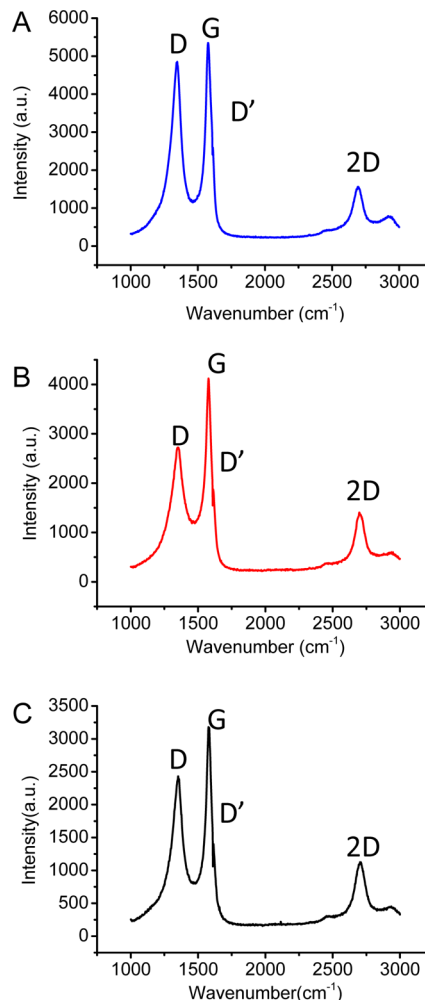


Figure 3. Raman spectra of boron-doped graphenes: doping level (A) 23 ppm, (B) 140 ppm, and (C) 590 ppm of B.

XPS, it provides further insight to the composition and bonding character of graphene sheets. 23 ppm B-G contained 82.48 atom % of C, 10.04 atom % of H, and 7.48 atom % of O; 140 ppm B-G contained 82.28 atom % of C, 10.03 atom % of H, and 7.69 atom % of O; 590 ppm B-G contained 84.83 atom % of C, 9.63 atom % of H, and 5.54 atom % of O. In addition, no nitrogen was found in any sample.

The electrical resistivity of the resulting boron-doped materials was studied by four point measurements of compressed tablets manufactured from the materials. The electrical resistivity of 13 ppm B-G was of 9.5×10^{-5} Ω·cm, of 140 ppm B-G 2.1×10^{-5} Ω·cm, and of 590 ppm B-G 2.3×10^{-4} Ω·cm. As can be observed from these results, higher content of boron in graphenes increases the electrical resistivity which is in accordance with the electron acceptor properties of boron.

The electrocatalytic activity of the prepared boron-doped graphenes toward oxygen reduction reaction (ORR) was investigated. We recorded cyclic voltammograms in both air and N₂ saturated 0.1 M KOH aqueous solution at three boron-doped surfaces. It is possible to observe significant reduction peak ~ -460 mV for air saturated KOH solution; no observable electrochemical reduction took place in N₂-saturated KOH solution. This signifies that the reduction peak ~ -460 mV is indeed originating from the reduction of oxygen. Cyclic voltammograms recording reduction of oxygen on boron-

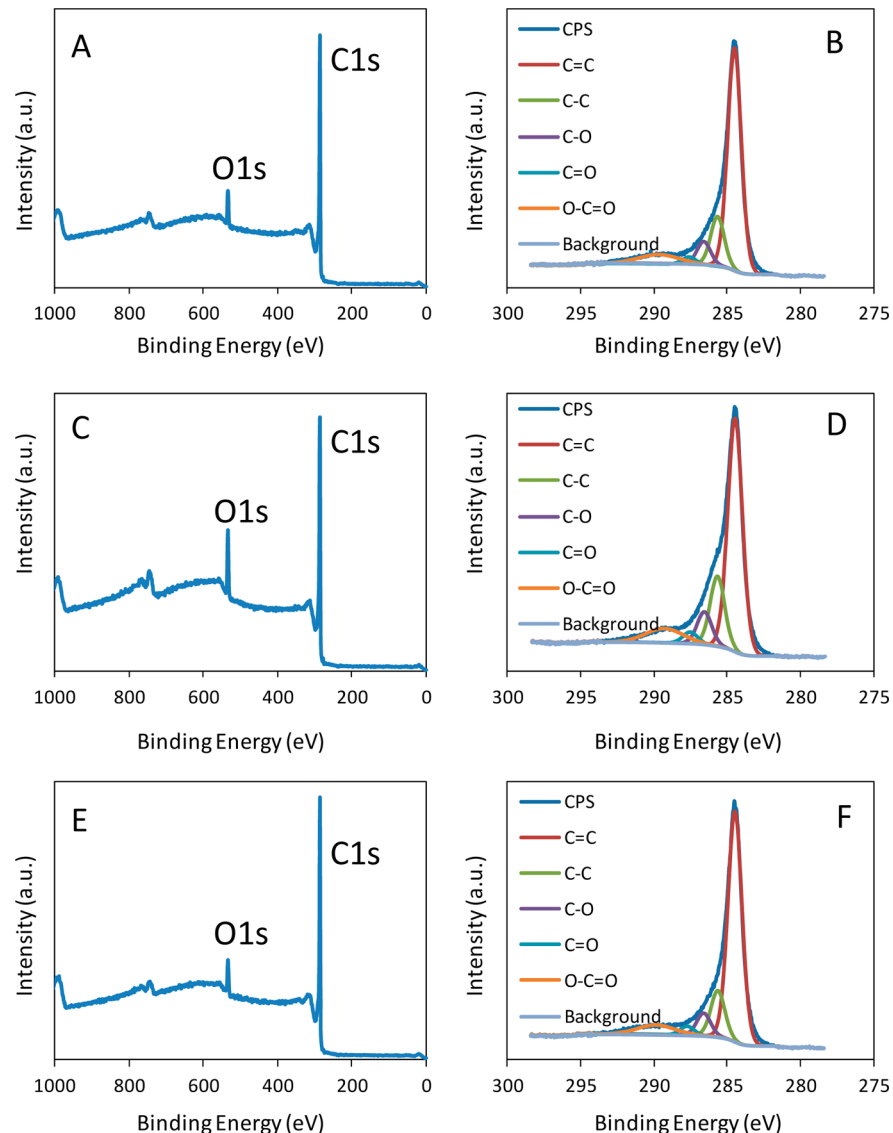


Figure 4. (Left) Wide-scan X-ray photoelectron spectra of boron-doped graphenes. (Right) C 1s high-resolution X-ray photoelectron spectra of boron-doped graphenes. Doping level (A,B) 23 ppm, (C,D) 140 ppm, and (E,F) 590 ppm of B.

doped graphenes with different doping levels, bare GC in 0.1 M KOH solution are shown in Figure 5. It is clear that the reduction peak shifts to increasingly negative potentials for the graphenes that contain increasing concentrations of boron dopant. Therefore, the more boron atoms doped, the lower the

electrocatalytic activity toward oxygen reduction for boron-doped graphene. This is in agreement with the general concept of hole-doping electrochemistry,²¹ but in contrast to some of the previous observations.¹² It should also be noted that the above-mentioned articles on oxygen reduction on boron-doped graphenes did not compare graphenes with different boron content.

We determined the weight-specific capacitance of boron-doped graphenes using cyclic voltammetry capacitive charge-discharge current, and the capacitance can be expressed as

$$C = \frac{I}{\nu} \quad (2)$$

where C is capacitance (F), I is current (A), and ν is the scan rate (mV/s, can be expressed as dE/dt).²²

The capacitances of boron-doped graphenes were investigated by measuring the current at an applied potential of 0.15 V with scan rates of 25, 50, 75, 100, 200, and 400 mV/s. As shown in Figure 6, the weight-specific capacitances of boron-doped graphene prepared at 1000 °C in N_2/H_2 , 800 °C in N_2 , and 1000 °C in N_2 are 11.6, 10.7, and 10.3 F/g, respectively, which

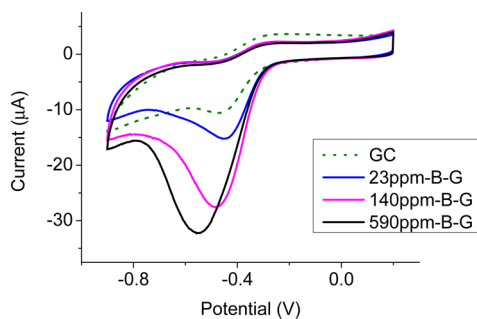


Figure 5. Oxygen reduction reaction performed in air saturated 0.1 M KOH buffer of three types of boron-doped graphenes and bare GC electrode. Conditions: scan rate 100 mV/s.

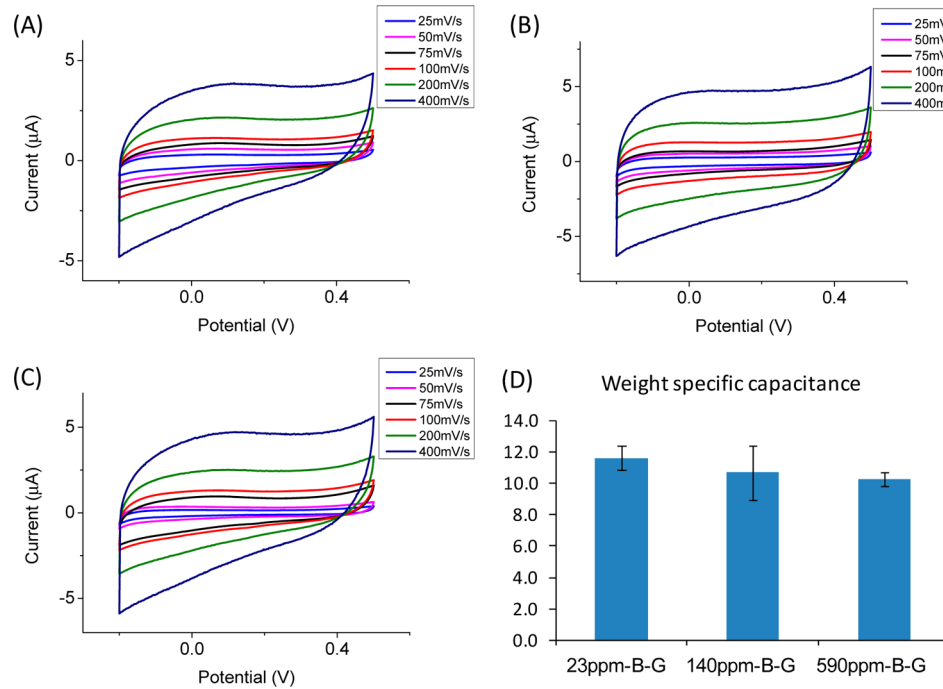


Figure 6. Weight-specific capacitance measured at scan rates of 25, 50, 75, 100, 200, and 400 mV/s of boron-doped graphenes with doping level of (A) 23 ppm, (B) 140 ppm, and (C) 590 ppm of B. (D) Comparison of the weight-specific capacitance on the above-mentioned B-doped graphenes.

indicate a decreasing trend of weight-specific capacitance with an increasing amount of doped boron atoms. Again, this is contrary to previous claims where B-doped graphenes¹¹ (and N-doped graphenes as well²³) demonstrated higher capacitance than nondoped counterparts. It should be noted that there is no theoretical background explanation, while in both cases, hole and electron doping, one should expect enhanced capacitance. The method used in mentioned paper by Han et al.¹¹ is based on hydroboration reaction well-known from organic chemistry. From the mechanism of such reaction, we can suppose formation of sp^3 -hybridized carbon with covalently bonded BH_2 group to the graphene backbone. It is not possible to obtain direct substitution of carbon with boron by the methods presented in Han et al.¹¹

CONCLUSIONS

We report a scalable method for tunable doping of boron atoms into the graphene framework via thermal exfoliation in an atmosphere with boron trifluoride diethyl etherate at various temperatures. The increasing amount of boron in doped graphenes leads to increasingly larger negative potentials needed for oxygen reduction reaction. This is in agreement with theory, where p-doped materials are expected to demonstrate lower electrocatalytic abilities in reduction reactions. In similar fashion, doping with higher concentrations of boron leads to a decrease in capacitance of the resulting materials.

EXPERIMENTAL SECTION

Materials. Sulfuric acid (98%), nitric acid (fuming, 98%), hydrochloric acid (37%), barium nitrate (99.5%), silver nitrate (99.5%), and potassium chlorate (98%) were purchased from PENTA, Czech Republic. Graphite microparticles (<50 μ m) were purchased from KOOH-I-NOOR Graphite, Czech Republic. Boron trifluoride diethyl etherate, potassium ferrocyanide, potassium hydroxide, *N,N*-dimethylformamide (DMF), sodium phosphate dibasic, potassium phosphate monobasic,

sodium chloride, and potassium chloride were purchased from Sigma-Aldrich. Nitrogen of 99.999% purity and hydrogen of 99.999% purity were obtained from SIAD, Czech Republic. Glassy carbon electrodes of 3 mm diameter were purchased from CH Instruments, TX.

Apparatus. A JEOL 7600F field emission scanning electron microscopy (JEOL, Japan) was used to obtain SEM images. A confocal micro-Raman LabRam HR instrument from Horiba Scientific in backscattering geometry with a CCD detector, a 514.5 nm Ar laser, and a 100 \times objective lens that was mounted on an Olympus optical microscope were used to measure the Raman spectra of the samples. The calibration is made by using a silicon reference with a peak position at 520 cm^{-1} and a resolution less than 1 cm^{-1} . X-ray photoelectron spectroscopy (XPS) samples were prepared by compacting a uniform layer of the materials on a carbon tape. A monochromatic Mg X-ray radiation source (SPECS, Germany) and a Phoibos 100 spectrometer are implemented to measure the survey and high-resolution C 1s, O 1s, and B 1s spectra. All voltammetric experiments were carried out by an Autolab PGSTAT101 electrochemical analyzer (Eco Chemie, The Netherlands). Electrochemical experiments were performed in a voltammetric cell (5 mL) at room temperature by using a three-electrode configuration. A glassy carbon electrode was used as working electrode, a platinum electrode as auxiliary electrode, and an Ag/AgCl electrode as a reference electrode. All electrochemical potentials are reported versus the Ag/AgCl electrode.

The combustible elemental analysis was performed with CHN PE 2400 Series II from Perkin-Elmer (USA). In CHN operating mode (the most robust and interference free mode), the instrument employs a classical combustion principle to convert the sample elements to simple gases (CO_2 , H_2O , and N_2). The PE 2400 analyzer performs automatically combustion and reduction, homogenization of product gases, separation, and detection. A microbalance MX5 (Mettler Toledo) is used for precise weighing of samples (1.5–2.5 mg per single sample

analysis). The accuracy of CHN determination is better than 0.30% abs. Internal calibration was performed using N-phenylurea.

Prompt γ -ray analysis (PGAA) was used to determine boron content in the graphene samples. These PGAA measurements were performed the PGAA facility which is installed at LWR-15 nuclear reactor.²⁴ The samples were irradiated in thermal neutron beam with flux $\sim 3 \times 10^6$ n cm⁻² s⁻¹. The gamma spectra were taken with the well-shielded 25% HPGe detector.

For electrical resistivity measurements of graphene materials, 40 mg of the powder material was first compressed into a capsule (1/4 in. diameter) under a pressure of 400 MPa for 30 s. The resistivity of the resulting capsule was measured by a 4-probe technique using the Van der Pauw method.²⁵ The resistivity measurements were then performed with Keithley 6220 current source and Agilent 34970A data acquisition/switch unit. The measuring current was set to 10 mA.

Procedures. Graphite Oxide Synthesis. The graphite oxide was prepared by Staudenmaier method²⁶ by adding 27 mL of nitric acid (fuming, 98%) and 87.5 mL of sulfuric acid (98% concentration) to a reaction flask which containing a magnetic stir bar. Then 5 g of graphite was added when the mixture was cooled to 0 °C. In order to get the homogeneous dispersion and avoid agglomeration, the mixture was vigorously stirred. 55 g of potassium chlorate was slowly added to the mixture while the flask was at 0 °C. When the added potassium chlorate was completely dissolved, the reaction flask was loosely capped to allow the gas that evolved during the reaction to escape. The mixture was kept stirring for 72 h at room temperature and when the reaction was finished, the mixture was poured into 3 L of distilled water and decanted. The formed graphite oxide was dispersed in HCl (5%) solutions in order to remove sulfate ions. Then the graphite oxide was repeatedly centrifuged and redispersed into distilled water until a negative reaction on chloride and sulfate ions (with AgNO₃ and Ba(NO₃)₂, respectively) was achieved. Finally, the graphite oxide was dried at 50 °C for 48 h in a vacuum oven before use.

Synthesis of Boron-Doped Graphene. The prepared graphite oxide was used as starting material and boron trifluoride diethyl etherate (BF₃Et₂O) as a boron precursor. The bubbler filled with liquid precursor was used for exfoliation at 20 °C and 1000 mbar. Nitrogen with flow rate of 100 mL/min was used as a carrier gas and was diluted with 1 L/min of nitrogen and a hydrogen/nitrogen mixture (0.5 L/min N₂ and 0.5 L/min H₂). The reactor was kept flushed with nitrogen. The flow of boron precursor was stabilized for 5 min before transferring of sample to the hot zone of the reactor, and then the exfoliation was carried out for 12 min at 800 and 1000 °C.

Cyclic Voltammetry. Cyclic voltammetry experiments were carried out at a 5 mL voltammetric cell at room temperature. Graphene materials were prepared in DMF in a concentration of 1 mg/mL and sonicated for 5 min and 1 μ L of the suspension was dropped onto the GC electrode, which was renewed by polishing with 0.05 μ m alumina particles on a polishing pad and washed with deionized water. The suspension on GC electrode was allowed to dry at room temperature. The weight-specific capacitance (C_w) was devised from the amount of graphene-related material deposited on the GC electrode.

AUTHOR INFORMATION

Corresponding Author

*E-mail: pumera@ntu.edu.sg. Fax: (65)6791-1961; Phone: (65) 6316-8796.

Notes

The authors declare no competing financial interest.

ACKNOWLEDGMENTS

M.P. thanks the NAP fund. Z.S. and P.Š. were supported by the Ministry of Education of the Czech Republic by the Specific University Research grant (MSMT no. 20/2013). Measurements of PGAA were carried out at the CANAM infrastructure of the NPI ASCR Rez supported by the Ministry of Education, Youth and Sports (grant project no. LM2011019).

REFERENCES

- (1) Rao, C. N. R.; Sood, A. K.; Subrahmanyam, K. S.; Govindaraj, A. Graphene: The New Two-Dimensional Nanomaterial. *Angew. Chem., Int. Ed.* **2009**, *48*, 7752–7777.
- (2) Wu, Z. S.; Ren, W.; Xu, L.; Li, F.; Cheng, H. M. Doped Graphene Sheets as Anode Materials with Superhigh Rate and Large Capacity for Lithium Ion Batteries. *ACS Nano* **2011**, *5*, 5463–5471.
- (3) Jin, Z.; Yao, J.; Kittrell, C.; Tour, J. M. Large-Scale Growth and Characterizations of Nitrogen-Doped Monolayer Graphene Sheets. *ACS Nano* **2011**, *5*, 4112–4117.
- (4) Reddy, A. L. M.; Srivastava, A.; Gowda, S. R.; Gullapalli, H.; Dubey, M.; Ajayan, P. M. Synthesis of Nitrogen-doped Graphene Films for Lithium Battery Application. *ACS Nano* **2010**, *4*, 6337–6342.
- (5) Velez-Fort, E.; Mathieu, C.; Palleggi, E.; Pigneur, M.; Silly, M. G.; Belkhou, R.; Marangolo, M.; Shukla, A.; Sirotti, F.; Ouerghi, A. Epitaxial Graphene on 4H-SiC(0001) Grown under Nitrogen Flux: Evidence of Low Nitrogen Doping and High Charge Transfer. *ACS Nano* **2012**, *6*, 10893–10900.
- (6) Qu, L.; Liu, Y.; Baek, J.-B.; Dai, L. Nitrogen-Doped Graphene as Efficient Metal-Free Electrocatalyst for Oxygen Reduction in Fuel Cells. *ACS Nano* **2010**, *4*, 1321–1326.
- (7) Gou, X. L.; Li, R.; Wei, Z. D.; Xu, W. Phosphorus-Doped Graphene Nanosheets as Efficient Metal-Free Oxygen Reduction Electrocatalysts. *RSC Adv.* **2013**, *3*, 9978–9984.
- (8) Panchakarla, L. S.; Subrahmanyam, K. S.; Saha, S. K.; Govindaraj, A.; Krishnamurthy, H. R.; Waghmare, U. V.; Rao, C. N. R. Synthesis, Structure, and Properties of Boron- and Nitrogen-Doped Graphene. *Adv. Mater.* **2009**, *21*, 4726–4730.
- (9) Wang, Y.; Shao, Y. Y.; Matson, D. W.; Li, J. H.; Lin, Y. H. Nitrogen-Doped Graphene and Its Application in Electrochemical Biosensing. *ACS Nano* **2010**, *4*, 1790–1798.
- (10) Sheng, Z. H.; Gao, H. L.; Bao, W. J.; Wang, F. B.; Xia, X. H. Synthesis of Boron Doped Graphene for Oxygen Reduction Reaction in Fuel Cells. *J. Mater. Chem.* **2012**, *22*, 390–395.
- (11) Han, J.; Zhang, L. L.; Lee, S.; Oh, J.; Lee, K.-S.; Potts, J. R.; Ji, J.; Zhao, X.; Ruoff, R. S.; Park, S. Generation of B-Doped Graphene Nanoplatelets Using a Solution Process and Their Supercapacitor Applications. *ACS Nano* **2013**, *7*, 19–26.
- (12) Choi, C. H.; Chung, M. W.; Kwon, H. C.; Park, S. H.; Woo, S. I. B.; N- and P, N-Doped Graphene as Highly Active Catalysts for Oxygen Reduction Reactions in Acidic Media. *J. Mater. Chem. A* **2013**, *1*, 3694–3699.
- (13) Archer, M. D. in *Nanostructured and Photoelectrochemical Systems for Solar Photon Conversion*; Nozik, A. J., Ed.; Imperial College Press: London, 2003; Vol. 3, pp 91.
- (14) Tryk, D. A.; Fujishima, A.; Honda, K. Recent Topics in Photoelectrochemistry: Achievements and Future Prospects. *Electrochim. Acta* **2000**, *45*, 2363–2376.
- (15) Kavan, L. Electrochemistry of Titanium Dioxide: Some Aspects and Highlights. *Chem. Rec.* **2012**, *12*, 131–142.
- (16) Schniepp, H. C.; Li, J.; McAllister, M. J.; Sai, H.; Herrera-Alonso, M.; Adamson, D. H.; Prud'homme, R. K.; Car, R.; Saville, D. A.; Aksay, I. A. Functionalized Single Graphene Sheets Derived from Splitting Graphite Oxide. *J. Phys. Chem. B* **2006**, *110*, 8535–8539.
- (17) McAllister, M. J.; Li, J.; Adamson, D. H.; Schniepp, H. C.; Abdala, A. A.; Liu, J.; Herrera-Alonso, M.; Milius, D. L.; Car, R.; Prud'homme, R.

- K.; Aksay, I. A. Single Sheet Functionalized Graphene by Oxidation and Thermal Expansion of Graphite. *Chem. Mater.* **2007**, *19*, 4396–4404.
- (18) Barroso-Bujans, F.; Alegria, A.; Colmenero, J. Kinetic Study of the Graphite Oxide Reduction: Combined Structural and Gravimetric Experiments under Isothermal and Nonisothermal Conditions. *J. Phys. Chem. C* **2010**, *114*, 21645–21651.
- (19) Sofer, Z.; Simek, P.; Pumera, M. Complex Organic Molecules are Released During Thermal Reduction of Graphite Oxides. *Phys. Chem. Chem. Phys.* **2013**, *15*, 9257–9264.
- (20) Cançado, L. G.; Takai, K.; Enoki, T.; Endo, M.; Kim, Y. A.; Mizusaki, H.; Jorio, A.; Coelho, L. N.; Magalhaes-Paniago, R.; Pimenta, M. A. General Equation for the Determination of the Crystallite Size L_a of Nanographite by Raman Spectroscopy. *Appl. Phys. Lett.* **2006**, *88*, 163106–163109.
- (21) Gratzel, M. Photoelectrochemical Cells. *Nature* **2001**, *414*, 338–344.
- (22) Li, J.; Cassell, A.; Delzeit, L.; Han, J.; Meyyappan, M. Novel Three-Dimensional Electrodes: Electrochemical Properties of Carbon Nanotube Ensembles. *J. Phys. Chem. B* **2002**, *106*, 9299–9305.
- (23) Zhang, L. L.; Zhao, X.; Ji, H.; Stoller, M. D.; Lai, L.; Murali, S.; McDonnell, S.; Cleveger, B.; Wallace, R. M.; Ruoff, R. S. Nitrogen Doping of Graphene and Its Effect on Quantum Capacitance, and a New Insight on the Enhanced Capacitance of N-doped Carbon. *Energy Environ. Sci.* **2012**, *5*, 9618–9625.
- (24) Honzátko, J.; Tomandl, I. Boron Concentration Measurements System for the Czech BNCT Project. In *Proceedings 10th International Symposium on Capture Gamma-Ray Spectroscopy and Related Topics, Santa Fe*, 1999; AIP 529; American Institute of Physics: New York, 2000; pp 749–750.
- (25) Van der Pauw, L. J. A Method of Measuring Specific Resistivity and Hall Effect of Discs of Arbitrary Shape. *Philips Res. Rep.* **1958**, *13*, 1–9.
- (26) Staudenmaier, L. Verfahren zur Darstellung der Graphitsäure. *Ber. Dtsch. Chem. Ges.* **1898**, *31*, 1481–1487.